Biochimica et Biophysica Acta, 1184 (1994) 45–53

BBABIO 43956

Pico- and nanosecond fluorescence kinetics of Photosystem II reaction centre and its complex with CP47 antenna

Arvi Freiberg [a,*], Kõu Timpmann [a], Andrei A. Moskalenko [b] and Nina Yu. Kuznetsova [b]

[a] *Institute of Physics, Estonian Academy of Sciences, Riia 142, EE2400 Tartu (Estonia) and*
[b] *Institute of Soil Sciences and Photosynthesis, Russian Academy of Sciences, 142292 Pushchino (Russia)*

(Received 26 March 1993)

Key words: Photosystem II; Reaction center; Light-harvesting antenna; Charge separation; Charge recombination; Energy and electron transfer; Fluorescence kinetics

Spectrally resolved pico- and nanosecond fluorescence kinetics of two types of Photosystem II core complex: D1/D2/cyt *b*559 reaction centres (RCs) and RCs together with CP47 proximal antenna have been studied at room temperature and at 77 K. The kinetics at room temperature were measured with the RCs being in different functional states. In the photoactive RCs at room temperature a picosecond decay with the lifetime components 13 ± 3 ps and 110 ± 30 ps is followed by the complex nanosecond kinetics. In the case of RC + CP47 complexes picosecond decays are slower: 25 ± 10 ps and 190 ± 30 ps, but nanosecond decay has similar behaviour. The data are analyzed by a simple three-state kinetic model postulating the formation of the primary radical pair in an unrelaxed form and allowing a back-recombination from that state. If this is correct, it is the proof that in the charge-separated state nuclear coordinate relaxation takes place on the picosecond time-scale. The following conclusions considering the nature and temporal characteristics of light excitations have been made: (i) At room temperature excitations are in equilibrium between P680 and the accessory chlorophylls including CP47 antenna and, therefore, only the average trapping time could be observed. This time is equal to 13 ± 3 ps in RCs and 25 ± 10 ps in RC + CP47 complexes. (ii) All other decays at room temperature (except probably part of the 5 ± 0.5 ns component) are of a recombination origin and reflect complex relaxation of the metastable radical pair state. (iii) At low temperatures an energetically directed excitation transfer, qualitatively very similar to the one observed in the core antenna of some purple bacteria takes place. This energy transfer is relatively slow with an apparent transfer time 10–20 ps at 77 K. (iv) Not only P680, but also P^+680 and $Pheo^-$ are very efficient quenchers of excitations.

Introduction

Although the reaction centre (RC) of photosynthetic bacteria has long been isolated in a pure form and its structure and functioning have been determined, much is still to be understood about the RCs of oxygen-evolving systems. The relatively recent isolation [1,2] of a rather simple Photosystem II (PS II) core, containing D1, D2 and cytochrome (cyt) *b*-559 proteins and revealing a photochemical activity, has opened new perspectives. As D1 and D2 proteins possess significant sequence homology to L- and M-subunits of bacterial RCs and bind a minimal amount of chlorophyll *a* (Chl), pheophytin *a* (Pheo), and β-carotene molecules, this complex is believed to represent a PS II RC which has lost quinone electron acceptors during the isolation procedure. Lack of quinone acceptors disrupts the chain of normal photochemical reactions in the RC already after the primary charge separation step between the electron donor denoted by P680 (likely a Chl dimer) and the acceptor, Pheo. The primary radical pair, $P^+680Pheo^-$, lives no longer than about 50 ns at room temperature [3,4]. The recombination of the radical pair leads to a partial regeneration of the excited state of the donor, P^*680, the formation of its triplet state, P^T680 or ground state.

By now the primary charge separation and the subsequent recombination processes in PS II RCs in the pico- and nanosecond time-domain have been studied by a number of groups [3–13] by using both transient

* Corresponding author. Fax: +372 34 72227.

SSDI 0005-2728(93)E0157-L

fluorescence and transient absorption techniques. In addition, valuable information about excited state lifetimes at very low temperatures has been provided by hole-burning spectroscopy [14] (for a latest review, see [15]). However, it has been found difficult to interpret self-consistently all the kinetic data obtained. Presumably, one of the main reasons for it is rather a limited stability of early preparations of the D1/D2/cyt *b*-559 RC complexes isolated with detergent Triton X-100, when exposed to light [6]. This detergent disrupts energy transfer from the accessory Chls to the P680 [14,16]. Milder detergents and anaerobic conditions can considerably improve the stability of the complexes [6,17], but their inherent lability due to light-activated protein cleavage is preserved [11]. In the case of fluorescence measurements, also limited time resolution may be an obstacle, as all the experiments so far have been performed with a system response function that 20–30 times exceeds the excited primary donor lifetime. The latter is measured by using the transient absorption method on the RC complexes isolated with Triton X-100 [8] and by the hole-burning method [15] to be $\leqslant 3$ ps.

In the present work, the spectrally resolved pico- and nanosecond fluorescence decay kinetics of stabilized PS II D1/D2/cyt *b*-559 RCs were, for the first time, studied with RCs being in different functional states (photoactive or open state, P680Pheo, and two different types of closed state, P^+680Pheo and P680 $Pheo^-$). It is demonstrated that the change of the RC state likewise the spectral selectivity is essential for the unambiguous interpretation of the observed complex decay curves. Special emphasis was put on resolving picosecond kinetics. The potential time resolution was greatly improved in comparison with the previous measurements by using a synchroscan streak camera instead of a time-correlated single-photon-counting technique. In parallel, a presumably more intact PS II unit, which, in addition to D1/D2/cyt *b*-559 RC, comprises the CP47 proximal light-harvesting antenna pigment–protein (henceforth denoted as the RC + CP47 complex), was studied. The aim was to investigate what influence the adding of 12 antenna Chl molecules [19] to RC pigments would have on the excitation quenching (trapping) kinetics. Also, in this case kinetics were measured with RCs being in different functional states. Measurements with photoactive RCs have been performed at room temperature and at sufficiently low temperature (77 K) for energy transfer processes between the pigments to become evident [5,8–10,12,14].

Preliminary data of this study have been reported at the VIIth International Symposium on Ultrafast Processes in Spectroscopy (Bayreuth, Germany, Oct. 7–10, 1991) [20] and at the IXth International Congress on Photosynthesis (Nagoya, Japan, Aug. 30 – Sept. 4, 1992) [21].

Materials and Methods

Samples and handling. Pigment–protein complexes from spinach were purified by modified procedures which improve stability by the exchange of detergent Triton X-100 with β-lauryl maltoside (see, e.g., [6]). RC and RC + CP47 complexes were isolated simultaneously in the first purification column. First the RCs were eluted from the column with 100 mM NaCl in the buffer (50 mM Tris-HCl (pH 7.2)) which contained 2 mM β-lauryl maltoside. Then RC + CP47 complexes were eluted with 150 mM NaCl in the same buffer. In order to prevent aeration during all the procedures the buffer was bubbled with argon. The samples were stored in 10–15% (v/v) glycerol at 77 K. Before the measurements the samples were resuspended in glycerol until the optical absorbance of $\leqslant 0.3$ at 676 nm in a 1 mm cuvette was obtained.

At room temperature RCs show a typical absorption spectrum with the Q_y band maximum at 675 nm (see Fig. 1, as measured with a Hitachi spectrophotometer). This ensures, according to [6,7,11,17], that more than 90% of RCs are photochemically active. The RC + CP47 complexes have a similar spectrum with the Q_y absorption maximum at 676 nm and with characteristic differences in the Soret band (Fig. 1).

The closed RC state with reduced Pheo (state P680$Pheo^-$) is accumulated when the samples are pretreated with 10–20 mg/ml sodium dithionite ($Na_2S_2O_4$) and methyl viologen in light [1,2,10]. The addition of 0.2–0.3 mg/ml silicomolybdate (SiMo), which is supposed to stay at the quinone Q_A site and accept electrons from $Pheo^-$, under illumination results in the accumulation of the closed RC state with an oxidized primary donor, P^+680Pheo [2,17]. The samples recover fully after illumination when kept in darkness for several minutes.

The sample degradation effects, described in [6,17–19] and also observed in our experiments with a longer exposure, needed for the time-correlated single-photon-counting method, were minimized by using new amounts of suspension after measuring only a few decay curves. We have observed no shift of the fluorescence band maximum after this short series of measurements (absorption spectrum was not checked). Yet, the variability of the kinetic data from sample to sample was quite remarkable (which may be due to uncontrollable initial degradation, e.g., during adjustment operations).

Setup and data analysis. For time-resolved fluorescence measurements the samples in a closed quartz cuvette in the air or in a nitrogen immersion cryostat were excited front face by about 4 ps pulses from a Coherent mode-locked dye laser pumped at 76 MHz with a Nd-YAG laser. The excitation wavelength was fixed at 590 nm. The average intensity on the sample

surface was less than 60 mW/cm^2, i.e., low enough to allow P^+680 to be safely reduced between successive excitations. Also, triplet states should have enough time to decay in our semi-aerobic conditions [18]. A checking with 10 times lower pulse intensity and with 10 times lower pulse repetition rate revealed no differences and gave certain confidence that the observed effects were not due to accumulated triplet states. The spectral regions of interest were selected by two monochromators combined in the subtractive-dispersion geometry in order to avoid an excessive pulse broadening within the spectrometer. Picosecond emission kinetics were recorded by a Hamamatsu synchroscan streak camera with the instrument response function 18 ps (full width at half maximum (FWHM)). Typical recording time with the streak camera system was 30 s.

In order to measure nanosecond kinetics, the pulse repetition rate was reduced 10 times by a cavity-dumper and a time-correlated single-photon-counting apparatus with the instrument response function of 400 ps was used. The kinetics were analyzed as a sum of exponentials by using a deconvolution procedure with the actual instrument response function. In order to improve the confidence level of the results a number (up to 10) of decay curves, measured presumably in the same conditions, were analyzed and average decay constants were determined.

A setup with streak camera was used to measure also steady-state fluorescence spectra (in this case no high-frequency deflection voltage was applied).

Results

The steady-state spectra

The absorption spectra of RC and RC + CP47 complexes at room temperature are shown in Fig. 1. When

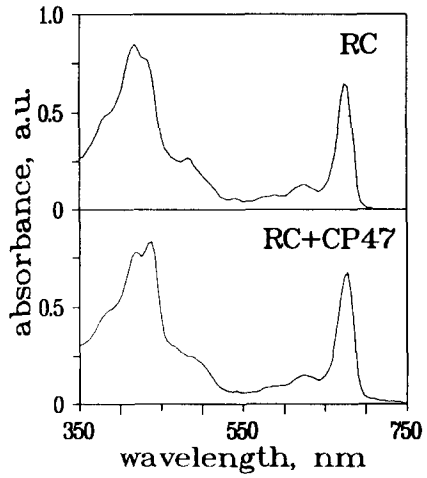

Fig. 1. Absorption spectra of the D1/D2/cyt *b*-559 RC and RC+CP47 complexes dissolved in glycerol at room temperature.

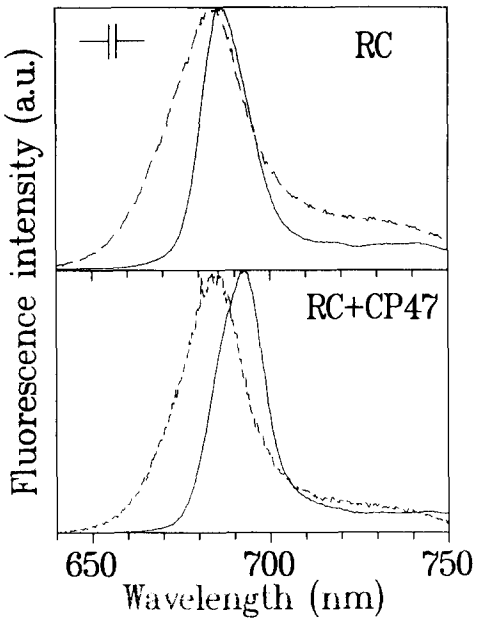

Fig. 2. Steady-state fluorescence spectra (uncorrected to apparatus response) of D1/D2/cyt *b*-559 RC and RC+CP47 complexes in glycerol at room temperature (dashed curves) and at 77 K (solid curves). Excitation at 590 nm. Recording bandwidth was 2 nm.

excited into the Q_x band at about 590 nm, the steady-state emission spectra (uncorrected to the apparatus spectral sensitivity) of both complexes have a single maximum at 684 nm, resonant to the Q_y absorption band, (Fig. 2). The addition of dithionite shifts the maximum by 2 nm to the blue side. The spectrum of RCs is much broader as compared to RC + CP47 complexes. This almost symmetric broadening may indicate a higher disorder presentage in less intact preparations as well as a larger amount of functionally uncoupled Chls. A comparison at low temperatures gives evidence that the latter reason is probably less significant in these preparations. At 77 K, the RC spectrum becomes nearly as narrow as the spectrum of RC + CP47, losing intensity mostly from its short-wavelength part. The maxima shift to 686 nm in the case of RCs and to 692 nm in the case of RC + CP47 complexes. In the latter case the fluorescence spectrum has a pronounced shoulder at about 686 nm, presumably due to RC pigments. When either sample is extensively treated with Triton X-100 or lithium dodecyl sulphate (LiDS), that are able to dissociate pigment–protein complexes to solubilized pigments and proteins, the fluorescence spectra at 77 K become similar and undergo a gradual blue-shift to about 675 nm. The absence of an apparent structure at this spectral range in our complexes is an indication of a reasonably small contribution of unconnected pigments. These steady-state spectral properties occur, as observed by others on similar preparations [6,22].

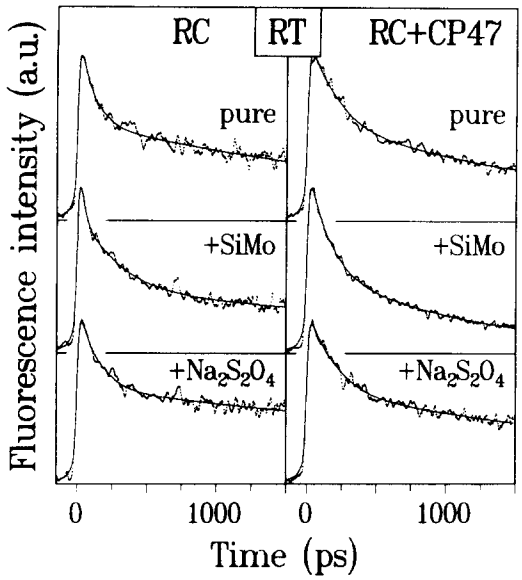

Fig. 3. Picosecond fluorescence kinetics of D1/D2/cyt *b*-559 RC and RC+CP47 complexes in glycerol with open and closed RCs at room temperature. Excitation at 590 nm. Recording at 683 nm with 16 nm bandwidth. Solid curves are multi-exponential fits to specific experimental data with the following lifetimes and relative amplitudes (in parentheses). Note that the nanosecond component represents a mixture of different components which cannot be resolved in this short fitting interval (see the next figure). RCs: 10 ps (0.6), 110 ps (1.2) and 4500 ps (1) (pure sample without chemical additives); 110 ps (1.8) and 2000 ps (1) (+SiMo); 90 ps (0.8) and 3700 ps (1) (+$Na_2S_2O_4$). RC+CP47 complexes: 30 ps (0.6), 190 ps (1.6) and 3100 ps (1) (pure); 150 ps (1.5) and 1500 ps (1) (+SiMo); 170 ps (1.0) and 3500 ps (1) (+$Na_2S_2O_4$).

Fluorescence kinetics at room temperature. Untreated samples

The picosecond time-resolved fluorescence kinetics at room temperature are shown in Fig. 3. The data for RCs and RC + CP47 complexes are represented side by side in order to underline the similarities or/and differences of their kinetic behaviour. The fluorescence kinetics were but weakly dependent on the emission wavelength in the range of 660–770 nm. Therefore, only the decay curves measured with low spectral resolution around the Q_y fluorescence band maximum are shown.

As one can see, in the case of untreated samples, where most of the RCs are expected to be in the photoactive P680Pheo state, the decays are clearly non-exponential. The initial picosecond-domain decay slows down and a substantial part of the emission has a nanosecond lifetime. No emission delay is observed. Fig. 4 follows the kinetics in the nanosecond time-domain, revealing an essential contribution of about 5 ns decay component. Earlier [6,7], a component with a similar lifetime was attributed to a functionally uncoupled Chl. Indeed, Triton X-100- or LiDS-treated samples show a single-exponential fluorescence decay with the 5.0 ± 0.5 ns lifetime (Fig. 4, bottom traces). The larger proportion of the 5 ns component in RC preparations with respect to RC + CP47 complexes might be due to a higher ratio of uncoupled pigments. However, this seems not to correlate with the steady-state spectral data as noted before.

When all the kinetics measured by a streak camera and a photomultiplier at room temperature were analyzed together with a fixed 5 ns decay, the following lifetimes (and relative amplitudes in parentheses) in the case of pure RCs could be extracted: 13 ± 3 ps (0.8), 110 ± 30 ps (1.6), 1.7 ± 0.2 ns (0.3), 5.0 ± 0.5 ns (1). The uncertainty in determining the relative amplitudes is not less than ±30%. The uncertainty limits represent the whole ensemble of data, not just a single kinetic curve. There are clearly presented also much slower (20–50 ns) components attributed to recombination luminescence in literature [5–7,10–12], which we have not measured accurately here. Their estimated total amplitude is about 1/10 of that of 5 ns compo-

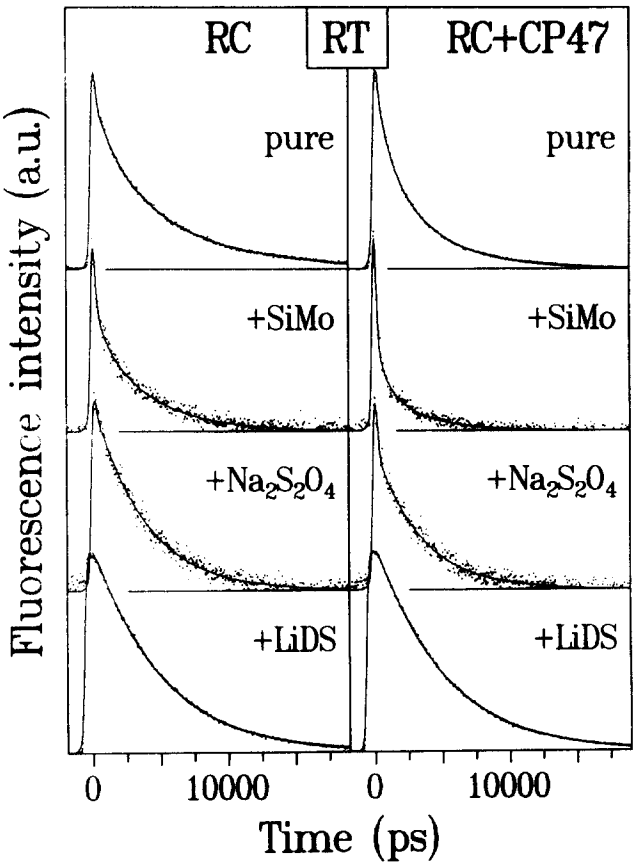

Fig. 4. The same as in Fig. 3, but measured with the single-photon-counting setup with the time scale expanded to nanos. Parameters of the fitting curves (with fixed 5 ns lifetime): RCs: 110 ps (2.6), 1550 ps (0.3) and 5000 ps (1) (pure); 140 ps (17.6), 3170 ps (4.3) and 5000 ps (1) (+SiMo); 100 ps (3.1), 3220 (1.2) and 5000 ps (1) (+$Na_2S_2O_4$); 5000 ps (+LiDS). RC+CP47 complexes: 150 ps (3.8), 1890 ps (1.7) and 5000 ps (1) (pure); 150 ps (13.5), 1060 ps (1.1) and 5000 ps (1)(+SiMo); 170 ps (5.3), 3120 (1.9) and 5000 ps (1) (+$Na_2S_2O_4$); 4900 ps (+LiDS).

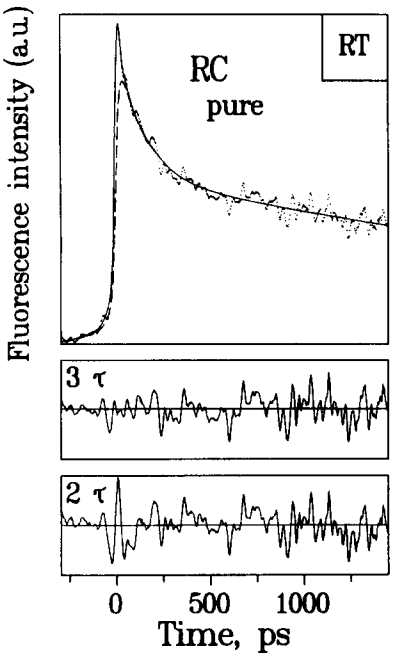

Fig. 5. Emission kinetics of RC complexes dissolved in the buffer without glycerol and reducing or oxidizing chemical additives at room temperature. Excitation and recording conditions were the same as in Fig. 3. Solid curve is the best computer-simulated fit with three exponentials: 7 ps (3.1), 139 ps (1.0) and 4680 ps (1). Dotted curve is the same with the 7 ps component subtracted. Lower parts of the figure demonstrate the approximation precision respectively for the three-exponential and the two-exponential fit. In the latter case the following parameters have been used: 110 ps (1.4) and 4850 (1).

nent. The yield of these components is a few times lower in more intact particles, which is in line with the biradical lifetime variation [4] and the change of efficiency for photoaccumulation of reduced Pheo [23], depending on the integrity of samples. On the short time-scale streak camera traces the 1.7 ns and 5.0 ns components form a slowly diminishing pedestal with an apparent intermediate decay time, depending on their relative amplitudes.

One should not, however, stick too much to the extracted lifetime values. As one will see later, they are good as an order-of-magnitude estimate of the time-scale of the systems dynamics and not all of them represent different dynamical processes. The used procedure of fitting by the sum of exponentials is a tradition, but in this case a clear oversimplification.

As it is evident from Fig. 3, the shortest picosecond component we were able to resolve in RC preparations was not shorter than 10 ps and constituted not more than about 1/3 of the initial amplitude of the picosecond signal. When the emission kinetics of RCs in the picosecond time range is approximated with a single decay constant, a characteristic lifetime of about 100 ps is obtained. We found (see Fig. 5) that when the pure buffer (i.e., without glycerol) was used as a solvent for RC preparations the initial fast fluorescence decay phase acquired most (3/4) of the amplitude, but the decay time remained (within the experimental accuracy) close to 10 ps. This dependence of the solvent deserves further characterization also for the RC + CP47 complex which was not investigated in buffer this time. Unfortunately, the samples dissolved in the buffer were found to be less stable and degrading already at room temperature when kept in darkness. This degradation expressed itself in the decrease of the overall fluorescence intensity as well as in the relative change of the amplitudes of different decay components. It was noted earlier [11] that at reduced levels of dodecyl maltoside the D1/D2 RCs tend to aggregate. An extensive aggregation was observed as a shortening of fluorescence lifetimes—an observation which is in line with our findings.

In RC + CP47 preparations the initial phase of the fluorescence decay is clearly slower than in RCs (see Fig. 3). It could be quite confidently approximated with two, 25 ± 10 ps (0.5) and 190 ± 30 ps (1.5), decay constants. (A single-exponential approximation gives the 200 ± 30 ps average lifetime.) Nanosecond components have lifetimes very similar to those in RCs.

Influence of the RC state

In the hope of relating the observed kinetic parameters to specific processes the functional state of the RCs at room temperature was changed. Apart from the loss of 20–50 ns recombination luminescence, which assures the intactness of our preparations, the major effect upon RC closure seems to be the relative increase of the amplitude of the picosecond kinetic component (see Fig. 4). This is especially remarkable in the case of the samples pretreated with SiMo. The latter may be due to a high quenching efficiency of an oxidized primary donor, as well as of partial oxidation of accessory pigments. In addition, it was recently established that in the presence of SiMo the oxidation of the accessory Chl results in its photodestruction [17]. A loss of antenna pigments may facilitate a faster picosecond emission decay of SiMo-treated RC + CP47 complexes as compared to pure preparations observable in Fig. 3. This problem will be discussed further below. In agreement with the observation in [10], there is a minor change of picosecond kinetics when Pheo is reduced to $Pheo^-$. Although the quenching mechanisms are still to be studied, our data support the opinion (see, e.g., [9]) that along P680, both P^+680 and $Pheo^-$ are very efficient excitation quenchers. When fitting the decay curves for pretreated samples in Fig. 4, we have assumed that chemical treatment has no or only minor influence on 5 ns decay time. This is probably not the case as far as the changed amplitude ratios and the appearance of a new intermediate decay component indicate.

Considering the 1.7 ± 0.2 ns decay component in pure samples, we only point to two observations: (i) this component is absent in pretreated samples and (ii) it has a relatively higher amplitude in more intact particles. This is the behaviour one would expect in case the 1.7 ns decay component is of a recombination luminescence origin.

Fluorescence kinetics at 77 K

The picosecond time-domain emission decay kinetics at 77 K are presented in Fig. 6. Only pure preparations have been studied at low temperature. Differently from the room temperature data, a very characteristic dependence on the emission wavelength is observed in both samples. At the blue edge of the fluorescence band the kinetics are dominated by a 15 ± 5 ps decay component. The accuracy of the measurements is not sufficient to decide whether there are shorter decay components than 10 ps, but, apparently, the initial fluorescence decay is faster and has a larger amplitude than it was on room temperature curves. The initial decay seems to be slightly slower in the case of RC + CP47 complexes. Besides the 15 ± 5 ps one a component with a lifetime around 100 ps can be resolved at the blue edge of the band. At longer wavelengths, the 15 ± 5 ps component decreases until it disappears at about 675 nm (in the case of RC) or at 680 nm (RC + CP47). At the same time slower picosecond component(s) gain in amplitude until the maximum is reached around 683 nm (RCs) or 684 nm (RC + CP47). One should emphasize that between 668–695 nm it is possible to fit the decays with the sum of exponentials, but the longer picosecond lifetime gradually increases from 100 ps to about 200 ps when recording at longer wavelengths. Further to the red these picosecond emissions also vanish, leaving apparently only the nanosecond pedestal which now reveals a 15–20 ps rise time. The amplitude spectrum of this nanosecond pedestal (its kinetics is unresolved in the experimental time-scale) has in RCs a maximum at 686 nm, which coincides with the peak of the steady-state fluorescence spectrum at 77 K. The same correlation holds in the case of RC + CP47 complexes, indicating that at low temperatures an essential fraction of excitations is trapped in the CP47 antenna system. In both cases these amplitude spectra show no structure and have only low intensity at 675 nm. This corresponds to a low concentration of uncoupled Chls and enforces the suggestion that the 5 ns decay component in untreated samples might have (at least partially) native (recombinational?) origin.

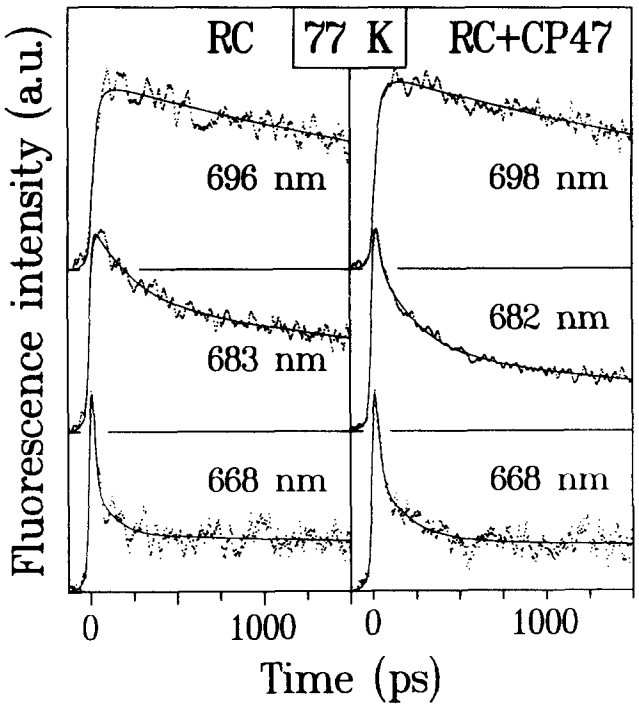

Fig. 6. Picosecond fluorescence kinetics of D1/D2/cyt *b*-559 and RC+CP47 complexes in glycerol at 77 K. Excitation at 590 nm. Recording at different indicated wavelengths with 4 nm bandwidth. Parameters of the fitting curves: RCs: 12 ps (7.5), 90 ps (2.0) and 9800 ps (1) (668 nm); 180 ps (0.7) and 3600 ps (1) (683 nm); 24 ps (−1) and 3550 ps (1) (696 nm). RC+CP47 complexes: 13 ps (4.8), 130 ps (2.3) and 5000 ps (1) (668 nm); 17 ps (1.3), 180 ps (1.4) and 2900 ps (1) (682 nm); 20 ps (−1.1), 710 ps (0.1) and 4500 ps (1) (698 nm).

Both the qualitative wavelength dependence of the observed picosecond fluorescence and even quantitative kinetics resemble what was measured in the antenna of photosynthetic bacteria [24,25]. Thus, by analogy, the observed kinetics may be interpreted as due to energetically downward-directed excitation transfer between accessory pigments towards P680. However, the apparent transfer rate in the PSII RC complexes is at variance with that in the bacterial RCs where two orders of magnitude larger transfer rates between accessory pigments and the primary donor have been estimated [26]. Yet, our slow energy transport data are not unique. They are well supported by photochemical hole-burning experiments at 1.6 K [14], where the energy transfer time from the accessory Chl to Pheo of 12 ps and from Pheo to P680 of 50 ps has been determined. Several other indications of slow energy transport at low temperatures (though not equally definite) have been published [5,8–10,12].

Discussion

Excited state dynamics in untreated samples at room temperature

Experimental data evidence that the apparent rate of excitation trapping in D1/D2/cyt *b*-559 RC particles is relatively slow as compared to the rate of

photoinduced oxidation of the primary donor. The latter process serves as an elementary mechanism for trapping and takes place, like in bacterial RCs [26], within less than 3 ps.

This paradox can be explained as follows. At room temperature thermal fluctuations (with the amplitude of the order of kT, i.e. $\simeq 210\ cm^{-1}$) can mix efficiently the almost isoenergetic (in comparison with the thermal energy kT) Q_y excited states of all the RC Chls and Pheos during their lifetime. Otherwise wavelength-dependent kinetics would be expected, but this was not observed at room temperature. This equilibrium excited state decays predominately by a photoinduced electron transfer mechanism from the excited P680 to Pheo, as proved by high quantum efficiency of the process. The macroscopic rate of excitation trapping, K_t, by the radical pair state with separated charges is in this case proportional to the microscopic charge separation rate, K_{cs}, and inversely proportional to the number of coupled pigments, N [27]:

$$K_t = K_{cs}/N. \tag{1}$$

Assuming $N \approx 8$ [19] and $K_{cs} \approx 2.8\ ps)^{-1}$ [8], it yields $K_t \approx (22\ ps)^{-1}$. For RC + CP47 particles with $N \approx 20$ a longer trapping time is expected, $K_t \approx (56\ ps)_{-1}$.

Qualitatively, a slow-down of the initial fluorescence decay with the antenna size was indeed observed in this work and has been noted before on larger PS II complexes [27–29]. However, the measured kinetics decay almost two times faster than predicted by this model. Also, the kinetics are not single-exponential. As shown below, this may be due to the recombination of the radical pair state, $P^+680\ Pheo^-$, back to excited primary donor state, P*680. Assuming the thermodynamic equilibrium between the states, the rate of the reverse reaction, K_{-t}, may be calculated by using the detailed balance condition and Eqn. 1 as

$$K_{-t} = K_{cs} \cdot \exp(-\Delta G/kT) \tag{2}$$

where ΔG is the free energy difference for the charge separation reaction and T is the absolute temperature. Note that the rates K_t and K_{-t} may in fact be quite similar, depending on N, ΔG and kT.

Let us consider the following simple three-level kinetic scheme

$$\xleftarrow{K_{11}} |1\rangle \underset{K_{-t}}{\overset{K_t}{\rightleftharpoons}} |2\rangle \xrightarrow{K_{22}}$$

where state $|1\rangle$ is the state with a photoexcited primary donor, P*680, in equilibrium with all excited accessory pigments and state $|2\rangle$ is the primary radical pair state, $P^+680Pheo^-$. The third state is the ground state. The following set of differential equations for the populations $n_1 = n(P^*680)$ and $n_2 = n(P^+680Pheo^-)$ can be written:

$$\begin{aligned} dn_1/dt &= -(K_{11} + K_t)n_1 + K_{-t}n_2 \\ dn_2/dt &= K_t n_1 - (K_{22} + K_{-t})n_2 \end{aligned} \tag{3}$$

Here K_{11} and K_{22} stand for all other decay channels except charge separation and recombination via state $|1\rangle$ and state $|2\rangle$, respectively. Population of state $|1\rangle$ and, consequently, the emission decay kinetics is then governed by the sum of two exponentials:

$$n_1 = C_1 \exp(-\lambda_1 t) + C_2 \exp(-\lambda_2 t) \tag{4}$$

with decay constants:

$$\lambda_{1,2} = \tfrac{1}{2}(K_t + K_{11} + K_{-t} + K_{22}) \pm \tfrac{1}{2}[(K_t + K_{11} + K_{-t} + K_{22})^2 - 4(K_{11}K_{-t} + K_{11}K_{22} + K_{22}K_t)]^{1/2}. \tag{5}$$

and the amplitude ratio:

$$C_1/C_2 = (K_{11} + K_t - \lambda_2)/(\lambda_1 - K_{11} - K_t).$$

Assuming $K_t \geqslant K_{-t} > K_{11} \gg K_{22}$, it follows that the faster decay constant is determined by the sum of the trapping and detrapping rate constants, $\lambda_1 \simeq K_t + K_{-t}$. The slower one has a limit $\lambda \simeq K_{11}/2$. Although the value of K_{11} is not reported, $\leqslant 10^9\ s^{-1}$ could be a right order-of-magnitude estimate from the long-wavelength kinetics at 77 K in Fig. 6. Thus, despite the reasonable value of λ_1, λ_2 does not suite the experiment in the picosecond time-domain. Another possible assumption, $K_t \geqslant K_{-t} > K_{22} \gg K_{11}$, gives $\lambda_1 \simeq K_t + K_{-t}$. This again does not explain the slower picosecond decay phase(s), if K_{22} is considered to represent the relaxed radical pair state with overall lifetime of a few tenths of nanoseconds [3,4].

Yet, there are several indications (both in plant and bacterial RCs) for the structural relaxation of protein surrounding in the (sub)nanosecond time-domain after the formation of the primary radical pair ([11,30,31], for reviews, see [32–34]). Proceeding from this possibility, the fluorescence decay kinetics were modelled based on rate equations (3) with free parameters ΔG and K_{22}.

A reasonable fitting of the experimental kinetics in the picosecond time range for both samples was obtained by using $\Delta G \simeq 0.05$ eV and $(K_{22})_{-1} \simeq 70$ ps. Other parameters were fixed as quoted before. Presumably, the concrete numbers, with respect to which the fitting procedure is rather sensitive, have little to do with any well-fixed state. However, the estimated values seem quite reasonable as, e.g., the free energy gap between P*680Pheo and the relaxed state of the primary radical pair at 277 K was previously calculated

to be 0.11–0.14 eV [11]. The same idea of a relaxing radical pair state could be employed further in order to explain also the later and slower phases of fluorescence kinetics. Considering the 0.5 ns lifetime component this was done in [11] where also $\Delta G \simeq 0.05$ eV was derived.

Thus, according to this (clearly oversimplified) homogeneous relaxation model, the lifetime and the amplitude of the fastest decay component reflect the trapping of the equilibrated excited state into the primary radical pair state. The slower picosecond component as well as all nanosecond components (except part of the 5 ± 0.5 ns component, which is due to the uncoupled Chls) may be of recombination luminescence (delayed fluorescence) origin.

Energy transfer between the pigments at 77 K

At 77 K the thermal excitation energy is substantially smaller than the bandwidth of an inhomogeneously broadened absorption spectrum. As expected in this case, a downward energy transfer from the short-wavelength excited Chl molecules towards the long-wavelength pigments is observed. This transfer causes the fastening of the short-wavelength fluorescence kinetics and, correspondingly, a delayed emission kinetics at longer wavelengths. The apparent transfer time of the order of 10 ps, is like in the bacterial antenna [24,25], but, as noted before, much two long in comparison with the estimated transfer between pigments in bacterial RCs [26]. The meaning of this difference needs to be understood. In [25], we made a guess that lifetimes of the order of 10 ps characterize excitation transport between different pigment–protein complexes. Within complexes the times are usually much shorter. Returning to PSII complexes, however, no substantial kinetic differences were observed in the case of RC and RC + CP47 complexes, in spite of their rather different composition. The excitations which escape photochemical trapping by P680, end up at the longest wavelength pigments and decay with a nanosecond decay time as shown in Fig. 6. The actual rate of trapping cannot be determined directly from the apparent kinetics around the fluorescence band maximum in Fig. 6, as at the present excitation conditions they are affected by a constant flow of higher-energy excitations toward P680. Long-lifetime pedestal at shorter wavelengths around 668 nm may include contribution from uncoupled Chls.

Concluding remarks

The experiments described have been self-consistently interpreted by a sequental relaxation model of the primary radical pair, quite analogous to the one in [11,30,31]. For the first time, relaxation in picosecond time-domain was observed. The following conclusions concern the nature and temporal characteristics of light excitations in PS II core complexes in pico- and nanosecond time-domain:

(i) During their lifetime at room temperature excitations reach equilibrium between P680 and accessory Chls, including CP47 antenna. Therefore, only the average trapping time (not the lifetime of P*680, as stated in [5,12,35]) can be observed. This time is equal to 13 ± 3 ps in RCs and 25 ± 10 ps in RC + CP47 complexes. The former number is in very good agreement with the recent absorption recovery times (13 ± 4 ps in [36] and < 21 ps in [13] (see discussion in [36])).

(ii) All other decays at room temperature (including part of the 5 ± 0.5 ns component) may be interpreted as of a delayed fluorescence origin due to back reactions that regenerate the excited state P*680 from the metastable radical pair states. As far as the delayed fluorescence kinetics reflects relaxation dynamics of the metastable radical pair state, the multi-exponential approach applied here should be considered only as the first approximation to the complex dynamical problem. For the same reason, the specific decay times determined, are good only as order-of-magnitude landmarks, not more.

(iii) At low temperatures an energetically directed excitation transfer, qualitatively very similar to the one observed in the core antenna of some purple bacteria, from the short-wavelength pigment forms towards the longer-wavelength ones takes place. This energy transfer is relatively slow with an apparent transfer time of the order of 10 ps at 77 K.

(iv) Not only P680, but also P^+680 and $Pheo^-$ are very efficient excitation quenchers.

Several very interesting problems underlined in the main text remain to be clarified. We share the opinion that both systems are awaiting a more extensive approach, as different dynamical processes in them cover an enormous time-span from 10^{-13} s to 10^{-1} s (this work is limited to about 10^{-11}–10^{-8} s).

Glasslike proteins are inhomogeneous systems and the relaxation processes in them are generally not adequately described by simple exponential kinetics. It is suggested that the relaxation in complex, slowly relaxing, strongly interacting materials follows the stretched exponential form, proportional to $\exp[-(t/\tau)^{\beta}]$, where $0 < \beta < 1$ [37]. Even when one forgets the influence of different protein conformations, there are still many reasons for heterogeneous kinetics: the macroscopic sample may consist of an ensemble of complexes with a different number of accessory Chls or/and an ensemble of complexes with changed charge separation rate (the long-debated α/β heterogeneity of PSII centres belongs here [35]). The fact that detergents, thus also the history of the sample, influence on these characteristics, has been well established [6,14,16]. The possibility of charge separation along either of the

two chromophore branches in RC should not be completely ignored as well [32].

The dynamics of the photoinduced radical pair state is poorly understood at present even in the case of generally much thoroughly studied bacterial RCs [31,32,34]. It has been proposed that fluctuations of the protein matrix contribute in the nanosecond time scale [31,34]. However, recent molecular dynamics studies of the *Rhodopseudomonas viridis* RC predict that protein stabilizes the separated electron pair state through dielectric relaxation very fast, within only 200 fs [38].

From the experimental point of view, further efforts to improve the temporal resolution of spontaneous fluorescence measurements are needed in order to cover the gap between the typical vibrational relaxation times in large molecules (10^{-13}–10^{-12} s) and much slower processes observed in this work.

Acknowledgements

The authors are indebted to Dr. T. Pullerits for valuable discussions and the help with computer modelling. Dr. T. Reinot is acknowledged for lending the photon counting setup and for technical assistance. Part of the manuscript was written during A.F.'s stay at the Department of Physics and Astronomy, Free University of Amsterdam. A.F. wishes to thank Prof. R. van Grondelle and his group for their kind hospitality and the Netherlands Organization for Scientific Research (NWO) for a visiting fellowship. Discussions with Dr. J. Dekker, Dr. P.J.M. van Kan and Mr. S. Kwa while writing the paper were most enlightening.

References

1 Namba, O. and Satoh, K. (1987) Proc. Natl. Acad. Sci. USA 84, 109–112.
2 Barber, J., Chapman, D.J. and Telfer, A. (1987) FEBS Lett. 220, 67–73.
3 Danielius, R.V., Satoh, K., Van Kan, P.J.M., Plijter, J.J., Nuijs, A.M. and Van Gorkom, H.J. (1987) FEBS Lett. 213, 241–244.
4 Hansson, O., Duranton, J. and Mathis, P. (1988) Biochim. Biophys. Acta 932, 91–96.
5 Mimuro, M., Yamazaki, I., Itoh, S., Tamai, N. and Satoh, K. (1988) Biochim. Biophys. Acta 933, 478–486.
6 Seibert, M., Picorel, R., Rubin, A.B. and Connolly, J.S. (1988) Plant Physiol. 87, 303–306.
7 Crystall, B., Booth, P.J., Klug, D.R., Barber, J. and Porter,G. (1989) FEBS Lett. 249, 75–78.
8 Wasielewski, M.R., Johnson, D.G., Govindjee, Preston, C. and Seibert, M. (1989) Photosynth. Res. 22, 89–99.
9 Van Kan, P.J.M., Otte, S.C.M., Kleinherenbrink, F.A.M., Nieveen, M.C., Aartsma, T.J. and Van Gorkom, H.J. (1990) Biochim. Biophys. Acta 1020, 146–152.
10 Govindjee, Van de Ven, M., Preston, C., Seibert, M. and Gratton, E. (1990) Biochim. Biophys. Acta 1015, 173–179.
11 Booth, P.J., Crystall, B., Ahmad, I., Barber, J., Porter, G. and Klug, D.R. (1991) Biochemistry 30, 7573–7586.
12 Roelofs, T.A., Gilbert, M. Shuvalov, V.A. and Holzwarth, A.R. (1991) Biochim. Biophys. Acta 1060, 237–244.
13 Durrant, J.R., Hastings, G., Hong, Q., Barber, J., Porter, G. and Klug, D.R. (1992) Chem. Phys. Lett. 188, 54–60.
14 Tang, D., Jankowiak, R., Seibert, M., Yocum, C.F. and Small,G.J. (1990) J. Phys. Chem. 94, 6519–6522.
15 Reddy, N.R.S., Lyle, P.A. and Small, G.J. (1992) Photosynth. Res. 31, 167–194.
16 Tang, O., Jankowiak, R., Seibert, M. and Small, G.J. (1990) Photosynth. Res. 27, 19–29.
17 Telfer, A., He, W.-Z. and Barber, J. (1990) Biochim. Biophys. Acta 1017, 143–151.
18 Durrant, J.R., Giorgi, L.B., Barber, J., Klug, D.R. and Porter, G. (1990) Biochim. Biophys. Acta 1017, 167–175.
19 Gounaris, K., Chapman, D.J., Booth, P., Crystall, B., Giorgi, L.B., Klug, D.R., Porter, G. and Barber, J. (1990) FEBS Lett. 265, 88–92.
20 Timpmann, K., Freiberg, A., Moskalenko, A.A. and Kuznetsova, N.Yu. (1992) in Ultrafast Processes in Spectroscopy 1991 (Laubereau, A. and Seilmeier, A., eds.), Institute of Physics Conference Series No. 126, IOP, Bristol, pp. 613–616.
21 Freiberg, A., Timpmann, K., Moskalenko, A.A. and Kuznetsova N.Yu. (1992) in Research in Photosynthesis, Vol. II (Murata, N., ed.), Kluwer Academic, Dordrecht, pp. 65–68.
22 Kwa, S.L.S., Newell, W.R., van Grondelle, R. and Dekker, J. (1992) Biochim. Biophys. Acta 1099, 193–202.
23 Barber, J. and Melis, A. (1990) Biochim. Biophys. Acta 1020, 285–289.
24 Timpmann, K., Freiberg, A. and Godik, V.I. (1991) Chem. Phys. Lett. 182, 617–622.
25 Freiberg, A., Timpmann, K. (1992) J. Photochem. Photobiol. B Biol. 15, 151–158.
26 Fleming, G.R., Martin, J.L. and Breton, J. (1988) Nature 333, 190–192.
27 Pearlstein, R.M. (1982) Photochem. Photobiol. 35, 835–844.
28 Schatz, G.H., Brock, H. and Holzwarth, A.R. (1988) Biophys. J. 54, 397–405.
29 Van Mieghem, F.J.E., Searle, G.F.W., Rutherford, A.W. and Schaafsma, T.J. (1992) Biochim. Biophys. Acta 1100, 198–206.
30 Schenck, C.C., Blankenship, R.E. and Parson, W.W. (1982) Biochim. Biophys. Acta 680, 44–59.
31 Woodbury, N.W.T. and Parson, W.W. (1984) Biochim. Biophys. Acta 767, 345–361.
32 Ogrodnik, A. (1990) Biochim. Biophys. Acta 1020, 65–71.
33 Renger, G. (1992) in The Photosystems: Structure, Function and Molecular Biology (Barber, J., ed.) Elsevier, pp. 45–99.
34 Goldstein, R.A. and Boxer, S.G. (1989) Biochim. Biophys. Acta 977, 78–86.
35 Holzwarth, A.R. and Roelofs, T.A. (1992) J. Photochem. Photobiol.B: Biol. 15, 45–62.
36 McCanley, S.W., Baranovski, A.P., Rice, J.K., Ghirardi, M.L. and Mattoo, A.K. (1992) Chem. Phys. Lett. 198, 437–442.
37 Palmer, R.G., Stein, D.L., Abrahams, E. and Anderson, P.W. (1984) Phys. Rev. Lett. 53, 958–961.
38 Treutlein, H., Schulten, K., Brünger, A.T., Karplus, M., Deisenhofer, J. and Michel, H. (1992) Proc. Natl. Acad. Sci. USA 89, 75–79.